



JULIUS-MAXIMILIANS-UNIVERSITÄT WÜRZBURG
INSTITUTE OF MATHEMATICS

WORKING GROUP ON NUMERICAL MATHEMATICS AND
APPLIED ANALYSIS

SUPERVISOR: DR. ELOI MARTINET

A Comparison of FEM and PINN with Variations of the Stokes Equation

Summer Term 2025

Christoph Roth and Florian Eich

Matr. No.: 3015984, 2458173

Master Mathematics

Email: christoph.roth@stud-mail.uni-wuerzburg.de,
florian.eich@stud-mail.uni-wuerzburg.de

July 18, 2025

Contents

1	Introduction	2
2	Mathematical Background	3
2.1	Preliminaries	3
2.2	Standard Stokes Flow	5
2.3	Stokes Flow with Inhomogeneous Boundary Conditions	9
2.4	Stokes Flow with Elliptical Obstacle	10
2.5	Lid-Driven Cavity	11
3	Finite Element Method	11
4	Physics-Informed Neural Networks	13
5	Comparison	14
6	Conclusion	18

1 Introduction

The numerical solution of partial differential equations (PDEs) plays an important role in applied mathematics, physics and engineering. Over the past decades, the *Finite Element Method (FEM)* has established itself as a robust and reliable tool for solving PDEs on complex geometries, particularly in fluid mechanics. Its success and popularity is not only grounded in a deep theoretical foundation but also in decades of algorithmic refinement.

On the contrary, in recent years, a different approach based on machine learning gained more and more attention, namely *Physics-Informed Neural Networks (PINNs)*. Unlike traditional solvers, this class of solution methods does not rely on mesh generation. Instead, PINNs represent the solution of a PDE as a neural network trained to minimize the residuals of the data-fitting, PDE and boundary loss.

This raises a number of important questions: Can these two fundamentally different approaches produce comparable results? Under which conditions is one preferable over the other? What are the trade-offs in terms of computational cost, accuracy and flexibility?

In this paper, we aim to address these questions through a systematic comparison of both FEM and PINNs applied to three classical benchmark flow problems induced by the Stokes equation: The standard Stokes flow with inhomogeneous boundary conditions, the Stokes flow around an (elliptical) obstacle and the Lid-Driven Cavity problem. Using the Python packages *FEniCS* for FEM and *PyTorch* for PINNs for each respective implementation, we consider a practical analysis of solution quality, convergence behavior and computational performance. The results provide insights into the strengths and limitations of both methods while also highlighting the role of the mathematical groundwork needed in order to implement them for such problems in the first place.

2 Mathematical Background

Before we can work with problems of this type, some preliminary work is needed. The aim of this section is to introduce and specify the notations, definitions and results of all necessary concepts. With this, we then want to derive the variational formulation of the Stokes problem and prove that each respective variation admits a unique solution under certain assumptions.

2.1 Preliminaries

In the following, let $\Omega \subset \mathbb{R}^n$ be an open domain with boundary $\partial\Omega$. Given a real Hilbert space H , we make use of $\langle \cdot, \cdot \rangle_H: H \times H \rightarrow \mathbb{R}$ and $\|\cdot\|_H: H \rightarrow \mathbb{R}$ to refer to the inner product and the induced norm in H , respectively. Considering a function $u: \Omega \rightarrow \mathbb{R}$, its *Laplacian* is given by

$$\Delta u := \partial_{11}^2 u + \dots \partial_{nn}^2 u,$$

where $\partial_{ij}^2 u := \frac{\partial^2 u}{\partial x_i \partial x_j}$ denotes the usual partial (second) derivative of u . In the more general case of partial derivatives, we use the following notation:

$$D^\alpha u := \frac{\partial^{|\alpha|} u}{\partial x^\alpha} := \frac{\partial^{\alpha_1 + \dots + \alpha_n} u}{\partial x_1^{\alpha_1} + \dots + \partial x_n^{\alpha_n}},$$

where $\alpha = (\alpha_1, \dots, \alpha_n) \in \mathbb{N}_0^n$. Further, for a multi-dimensional function $\sigma: \Omega \rightarrow \mathbb{R}^{n \times n}$, the *divergence* of σ is defined as

$$\operatorname{div}(\sigma) := \left(\sum_{j=1}^n \partial_j \sigma_{ij} \right)_{1 \leq i \leq n}.$$

Coming back to the class of functions represented by u , we define the corresponding *support* as the set $\operatorname{supp}(u) := \{x \in \Omega \mid u(x) \neq 0\}$. Building on that, we introduce

$$\mathcal{D}(\Omega) := C_c^\infty(\Omega) := \{\phi \in C^\infty(\Omega) \mid \operatorname{supp}(\phi) \subseteq \Omega \text{ is compact and } \operatorname{supp}(\phi) \cap \partial\Omega = \emptyset\},$$

with $C^\infty(\Omega) := \bigcap_{m \in \mathbb{N}} C^m(\Omega)$ as the vector space of *test functions* over Ω . One important Hilbert space we will need later on is the following.

Definition 2.1 (Lebesgue space) Given a nonempty set $\Omega \subset \mathbb{R}^n$, the associated *Lebesgue space* is denoted by

$$L^2(\Omega) := \{u: \Omega \rightarrow \mathbb{R} \mid u \text{ is measurable and } \|u\|_{L^2(\Omega)} < \infty\},$$

with the norm $\|u\|_{L^2(\Omega)} := \sqrt{\langle u, u \rangle_{L^2(\Omega)}}$, induced by the inner product

$$\langle u, v \rangle_{L^2(\Omega)} := \int_{\Omega} u(x)v(x) \, dx.$$

The fact that this space is indeed a Hilbert space is not hard to see. However, for the sake of simplicity, we do not provide an explicit proof but instead refer to [2, Theorem 2.6.15] for a deeper analysis.

Another concept which will play a crucial role in the elaborations to come is the one of *weak derivatives*.

Definition 2.2 (Weak derivative) Consider $u \in L^2(\Omega)$ and $\alpha \in \mathbb{N}_0^n$. We call u *weakly differentiable* if there exists $v_\alpha \in L^2(\Omega)$ satisfying

$$\langle v_\alpha, \phi \rangle_{L^2(\Omega)} = (-1)^{|\alpha|} \langle u, D^\alpha \phi \rangle_{L^2(\Omega)}$$

for every $\phi \in \mathcal{D}(\Omega)$. Consequently, v_α is referred to as the α -th *weak derivative* of u and we set $D^\alpha u = v_\alpha$.

Note that weak derivatives are unique. Using this, we now introduce another special Hilbert space.

Definition 2.3 (Sobolev space) Given a nonempty open set $\Omega \subset \mathbb{R}^n$ and $k \in \mathbb{N}_0$, the associated *Sobolev (Hilbert) space* of order k is given by

$$H^k(\Omega) := \{v \in L^2(\Omega) \mid \text{for every } \alpha \in \mathbb{N}_0^n \text{ with } |\alpha| \leq k, \text{ there exists (weak) } D^\alpha u \in L^2(\Omega)\},$$

with the associated inner product

$$\langle u, v \rangle_{H^k(\Omega)} := \sum_{|\alpha| \leq k} \langle D^\alpha u, D^\alpha v \rangle_{L^2(\Omega)}$$

and the induced norm

$$\|u\|_{H^k(\Omega)} := \left(\sum_{|\alpha| \leq k} \|D^\alpha u\|_{L^2(\Omega)}^2 \right)^{1/2}.$$

Using this norm, we denote the completion of the space of test functions by

$$H_0^k(\Omega) := \overline{\mathcal{D}(\Omega)}^{\|\cdot\|_{H^k(\Omega)}}$$

For every $k \in \mathbb{N}$, both $H^k(\Omega)$ and $H_0^k(\Omega)$ are Hilbert spaces with respect to the inner product introduced in the definition above. The next definitions and results introduce some well known concepts. Regardless of this and for the sake of completeness, we formally introduce them once again. However, since we will only make use of them as auxiliary results, we omit the corresponding proofs at this point and instead refer to [5, Theorem 2.1] for a further elaboration.

Definition 2.4 (Continuous linear form) Let V be a Hilbert space. We say that $L: V \rightarrow \mathbb{R}$ is a *continuous linear form* on V if it is linear and satisfies

$$|L(v)| \leq C \|v\|_V, \quad \forall v \in V,$$

for some $C > 0$.

Definition 2.5 (Continuous bilinear form) Let V be a Hilbert space. A mapping $a: V \times V \rightarrow \mathbb{R}$ is called *continuous bilinear form* if it is linear in both respective arguments and satisfies

$$|a(u, v)| \leq c_a \|u\|_V \|v\|_V, \quad \forall u, v \in V,$$

for some *continuity constant* $c_a > 0$.

Definition 2.6 (Coercivity) Let V be a Hilbert space. A mapping $a: V \times V \rightarrow \mathbb{R}$ is deemed *coercive* if it holds

$$|a(u, u)| \geq \nu \|u\|_V^2, \quad \forall u \in V,$$

for some *coercivity constant* $\nu > 0$.

Lemma 2.7 (Young's inequality) Consider two nonnegative real numbers $a, b \in \mathbb{R}_0^+$ and two real numbers $p, q > 0$ satisfying $\frac{1}{p} + \frac{1}{q} = 0$. Then, it holds

$$ab \leq \frac{a^p}{p} + \frac{b^q}{q}.$$

Lemma 2.8 (Green's first identity) Let $\Omega \subset \mathbb{R}^n$ be an open bounded set and consider two twice differentiable functions $u, v: \Omega \rightarrow \mathbb{R}^2$. Then, the following holds

$$\int_{\Omega} \nabla u : \nabla v = - \int_{\Omega} u \cdot \Delta v + \int_{\partial\Omega} u \cdot \frac{\partial v}{\partial n},$$

where $\nabla u : \nabla v := \sum_{i,j} \partial_j u_i \cdot \partial_j v_i$.

Lemma 2.9 (Poincaré inequality) Let $\Omega \subset \mathbb{R}^n$ be an open bounded set. Then, there exists some constant $C > 0$ such that

$$\|u\|_{L^2(\Omega)} \leq C \|\nabla u\|_{L^2(\Omega)}$$

for every $u \in H_0^1(\Omega)$.

We conclude this section by stating the main result on which the elaborations on the existence of solutions in the sections to follow are based on.

Theorem 2.10 (Lax-Milgram) Let V be a Hilbert space. On this space, consider a continuous linear form L as well as a continuous and coercive bilinear form a . Then, the following problem admits a unique solution

Find $u \in V$ such that $a(u, v) = L(v)$, for every $v \in V$.

2.2 Standard Stokes Flow

In this section, we want to introduce the basic problem on which all later problems we consider are based on, the so-called *standard Stokes (flow) problem*. In particular, we are going to derive the weak formulation and prove the existence and uniqueness of a solution.

For a given domain $\Omega \subset \mathbb{R}^2$, we want to find a pair (u, p) such that

$$-\mu \Delta u + \nabla p = f \quad \text{in } \Omega, \tag{1}$$

$$\operatorname{div}(u) = 0 \quad \text{in } \Omega, \tag{2}$$

$$u = 0 \quad \text{on } \partial\Omega,$$

where $u: \Omega \rightarrow \mathbb{R}^2$ can be interpreted as the *velocity field* of an incompressible fluid motion, $p: \Omega \rightarrow \mathbb{R}$ the *pressure field*, $f: \Omega \rightarrow \mathbb{R}$ a *source term* and $\mu > 0$ the *viscosity coefficient*

of the fluid.

For the derivation of the variational formulation, we now follow the usual approach. First, we define

$$\begin{aligned} V &:= (H_0^1(\Omega))^2 = \{v \in (H^1(\Omega))^2 \mid v = 0 \text{ on } \partial\Omega\}, \\ Q &:= L^2(\Omega), \end{aligned}$$

as the space of *test velocities* and the *pressure space*, respectively. We continue by multiplying a test function $v \in V$ to the *momentum equation* (1) and $q \in Q$ to the *mass equation* (2) to get

$$\begin{aligned} -\mu \Delta u \cdot v + \nabla p \cdot v &= f \cdot v, \\ \operatorname{div}(u) \cdot q &= 0. \end{aligned}$$

Integrating over Ω on both sides of each equation yields

$$-\mu \int_{\Omega} \Delta u \cdot v + \nabla p \cdot v = \int_{\Omega} f \cdot v, \quad (3)$$

$$\int_{\Omega} \operatorname{div}(u) \cdot q = 0. \quad (4)$$

In order to simplify the equation (3) we apply [Green's first identity](#) and use integration by parts. In practice, we get

$$\int_{\Omega} -\Delta u \cdot v = \int_{\Omega} \nabla u : \nabla v - \underbrace{\int_{\partial\Omega} \frac{\partial u}{\partial n} \cdot v}_{= 0 \text{ since } v \in V}. \quad (5)$$

For the pressure term, we now use integration by parts as well in order to see

$$\int_{\Omega} \nabla p \cdot v = - \int_{\Omega} p \cdot \operatorname{div}(v) + \underbrace{\int_{\partial\Omega} p \cdot v \cdot \vec{n}}_{= 0 \text{ since } v \in V}, \quad (6)$$

where \vec{n} is the normal vector to the boundary $\partial\Omega$. Now combining (3), (5) and (6), we arrive at the following expression for our moment equation

$$\mu \int_{\Omega} \nabla u : \nabla v - \int_{\Omega} p \cdot \operatorname{div}(v) = \int_{\Omega} f \cdot v. \quad (7)$$

With this, we define the following bilinear and linear forms

$$\begin{aligned} \tilde{a}(u, v) &:= \mu \int_{\Omega} \nabla u : \nabla v, \\ b(v, p) &:= - \int_{\Omega} p \cdot \operatorname{div}(v), \\ b(u, q) &:= - \int_{\Omega} q \cdot \operatorname{div}(u), \\ L(v) &:= \int_{\Omega} f \cdot v. \end{aligned}$$

Hence, we get the variational (saddle-point) problem: Find $(u, p) \in V \times Q$ such that

$$\tilde{a}(u, v) + b(v, p) = L(v) \quad \forall v \in V, \quad (8)$$

$$b(u, q) = 0 \quad \forall q \in Q. \quad (9)$$

Usually, we would mostly be done with the elaborations at this point. One would now show that this problem satisfies the *Brezzi conditions*, in particular the *Ladyzhenskaya-Babuška-Breezi condition* in order to get the existence and uniqueness of a solution (cf. [1, Chapter 4.2]). However, showing the latter condition often proves to be rather difficult, especially when it comes to finding compatible function spaces. As suggested in [4, Chapter 20.2.2], one may introduce a stabilization term for the pressure. This converts the saddle-point problem from above into a coercive problem, thereby avoiding the need for Brezzi's conditions and enabling the use of the much simpler [Lax-Milgram theorem](#). The pressure stabilizing term we consider here, is the following

$$\epsilon \int_{\Omega} p \cdot q,$$

for some $\epsilon > 0$. We combine this with (8) and (9) and get our final (stabilized) variational formulation: Find $(u, p) \in V \times Q$ such that for all $(v, q) \in V \times Q$

$$\underbrace{\tilde{a}(u, v) + b(v, p) + b(u, q) + \epsilon \int_{\Omega} p \cdot q}_{=: a((u, p), (v, q))} = L(v) \quad (10)$$

We now conclude this section on the Stokes problem with a formal proof of existence and uniqueness of a solution for our variational formulation.

Theorem 2.11 Let $V := H_0^1(\Omega)^2$ and $Q := L^2(\Omega)$. Then, the stabilized variational formulation (10) of the Stokes problem admits a unique solution for every $\epsilon > 2C^2/\mu$.

Proof. From the construction of a , we already get that it is a bilinear form on $W \times W$ with $W := V \times Q$ and the standard norm $\|(v, q)\|_W^2 = \|v\|_{H^1(\Omega)}^2 + \|q\|_{L^2(\Omega)}^2$. Note that, by definition, one has

$$\|v\|_{H^1(\Omega)} \leq \|(v, q)\|_W \quad \text{as well as} \quad \|q\|_{L^2(\Omega)} \leq \|(v, q)\|_W, \quad (11)$$

for every $(v, q) \in W$. In order to show continuity of a , we consider the following inequalities

$$\begin{aligned} \left| \mu \int_{\Omega} \nabla u : \nabla v \right| &\leq \mu \|\nabla u\|_{L^2(\Omega)} \|\nabla v\|_{L^2(\Omega)} \leq \mu \|u\|_{H^1(\Omega)} \|v\|_{H^1(\Omega)}, \\ \left| \int_{\Omega} p \cdot \operatorname{div}(v) \right| &\leq \|p\|_{L^2(\Omega)} \|\operatorname{div}(v)\|_{L^2(\Omega)} \leq C \|p\|_{L^2(\Omega)} \|v\|_{H^1(\Omega)}, \\ \left| \int_{\Omega} q \cdot \operatorname{div}(u) \right| &\leq \|q\|_{L^2(\Omega)} \|\operatorname{div}(u)\|_{L^2(\Omega)} \leq C \|q\|_{L^2(\Omega)} \|u\|_{H^1(\Omega)}, \\ \left| \epsilon \int_{\Omega} p \cdot q \right| &\leq \epsilon \|p\|_{L^2(\Omega)} \|q\|_{L^2(\Omega)}, \end{aligned}$$

derived using the Cauchy-Schwarz inequality and the fact that the divergence is a bounded operator in $H^1(\Omega)$. To see the latter, one may write the L^2 -norm in its integral form, consider the Cauchy-Schwarz inequality for the integrand and notice that it holds $\|u\|_{H^1(\Omega)}^2 = \|u\|_{L^2(\Omega)}^2 + \|\nabla u\|_{L^2(\Omega)}^2$ (cf. [Definition 2.3](#)). We now combine these estimates and apply the triangle inequality in order to get

$$\begin{aligned} |a((u, p), (v, q))| &\leq \max(\mu, \epsilon, C) \cdot (\|u\|_{H^1(\Omega)} + \|p\|_{L^2(\Omega)}) \cdot (\|v\|_{H^1(\Omega)} + \|q\|_{L^2(\Omega)}) \\ &\leq 4 \cdot \max(\mu, \epsilon, C) \cdot \|(u, p)\|_W \cdot \|(v, q)\|_W, \end{aligned}$$

where in the second inequality, we used (11). Hence, by [Defintion 2.5](#), we have that a is a continuous bilinear form on $W \times W$.

The next step now is to show coercivity of a . For this, consider some arbitrary but fixed $(u, p) \in V \times Q$. Then, one has

$$\begin{aligned} a((u, p), (u, p)) &= \mu \|\nabla u\|_{L^2(\Omega)}^2 - 2 \underbrace{\int_{\Omega} p \cdot \operatorname{div}(u)}_{\leq \|p\|_{L^2(\Omega)} \|\operatorname{div}(u)\|_{L^2(\Omega)}} + \epsilon \|p\|_{L^2(\Omega)}^2 \\ &\geq \mu \|\nabla u\|_{L^2(\Omega)}^2 - 2 \|p\|_{L^2(\Omega)} \|\operatorname{div}(u)\|_{L^2(\Omega)} + \epsilon \|p\|_{L^2(\Omega)}^2 \\ &\geq \mu \|\nabla u\|_{L^2(\Omega)}^2 - 2C \|p\|_{L^2(\Omega)} \|u\|_{H^1(\Omega)} + \epsilon \|p\|_{L^2(\Omega)}^2 \end{aligned} \quad (12)$$

where the first inequality is again a consequence of the Cauchy-Schwarz inequality and the second one uses the same estimation for the divergence operator as before. Now using the [Poincaré inequality](#), we further have

$$C_u \|\nabla u\|_{L^2(\Omega)}^2 \geq \|u\|_{L^2(\Omega)}^2,$$

for some $C_u > 0$. Adding $\|\nabla u\|_{L^2(\Omega)}^2$ on both sides yields

$$(1 + C_u) \|\nabla u\|_{L^2(\Omega)}^2 \geq \|u\|_{H^1(\Omega)}^2.$$

Applying this to (12) and using [Young's inequality](#) yields

$$\begin{aligned} a((u, p), (u, p)) &\stackrel{(12)}{\geq} \mu \|\nabla u\|_{L^2(\Omega)}^2 - 2C \|p\|_{L^2(\Omega)} \|u\|_{H^1(\Omega)} + \epsilon \|p\|_{L^2(\Omega)}^2 \\ &\geq \frac{\mu}{1 + C_u} \|u\|_{H^1(\Omega)}^2 - 2C \|p\|_{L^2(\Omega)} \|u\|_{H^1(\Omega)} + \epsilon \|p\|_{L^2(\Omega)}^2 \\ &\geq \frac{\mu}{1 + C_u} \|u\|_{H^1(\Omega)}^2 - \left(\frac{4C^2}{2\mu} \|p\|_{L^2(\Omega)}^2 + \frac{\mu}{2} \|u\|_{H^1(\Omega)}^2 \right) + \epsilon \|p\|_{L^2(\Omega)}^2 \\ &= \left(\frac{\mu}{1 + C_u} - \frac{\mu}{2} \right) \|u\|_{H^1(\Omega)}^2 + \left(\epsilon - \frac{2C^2}{\mu} \right) \|p\|_{L^2(\Omega)}^2 \\ &\geq \underbrace{\min \left(\frac{\mu - \frac{\mu}{2}}{1 + C_u}, \epsilon - \frac{2C^2}{\mu} \right)}_{=: \nu} \|(u, p)\|_W^2. \end{aligned}$$

Hence, a is coercive with coercivity constant ν for $\epsilon > 2C^2/\mu$.

The final step now consists of proving continuity of the right-hand side $L(v)$. Similar to the beginning of the proof, we use Cauchy-Schwarz in order to see

$$|L(v)| = \left| \int_{\Omega} f \cdot v \right| \leq \|f\|_{L^2(\Omega)} \|v\|_{L^2(\Omega)} \leq \|f\|_{L^2(\Omega)} \|v\|_{H^1(\Omega)}$$

for every $v \in V$. With this, we are now able to apply [Theorem 2.7](#) and have that there exists a unique solution $(u, p) \in V \times Q$ to our variational problem (10), thereby finishing the proof. \square

2.3 Stokes Flow with Inhomogeneous Boundary Conditions

We now come to the first practical variation of the standard Stokes problem introduced in the section before. Again, we will discuss the weak formulation and prove existence as well as uniqueness of a solution. Let $\Omega := (0, 1)^2 \subset \mathbb{R}^2$, $\mu := 1$ and again consider

$$\begin{aligned} -\mu \Delta u + \nabla p &= f & \text{in } \Omega, \\ \operatorname{div}(u) &= 0 & \text{in } \Omega. \end{aligned}$$

Instead of the initial boundary condition $u = 0$ on $\partial\Omega$, we now set the following *Dirichlet boundary conditions*

$$u = (1, 0)^T \quad \text{on } \Gamma_L, \tag{13}$$

$$u = (0, 0)^T \quad \text{on } \Gamma_W, \tag{14}$$

with $\Gamma_L := \{0\} \times (0, 1) \subset \partial\Omega$ and $\Gamma_W := (0, 1) \times \{0, 1\} \subset \partial\Omega$ denoting the left, top and bottom parts of the boundary $\partial\Omega$, respectively. The left boundary condition is often called *inflow* whereas the restriction for the top and bottom is referred to as *no-slip*. Note that we do not impose any boundary conditions on the right-hand side of the domain, i.e., we do restrict the *outflow* in any way.

In practice, the variational formulation itself does not differ from the one of the standard Stokes problem. Since we only modified the occurring boundary conditions which are implicitly embedded in corresponding function space of the velocity u , both the linear and bilinear form stay the same. The difficulty now lies in said function space since we cannot apply the same proof of existence and uniqueness right away. However, we will now introduce a trick that handles such inhomogeneous boundary conditions by splitting the velocity into two parts: Let $u_D \in H^1(\Omega)^2$ be given such that it is arbitrarily smooth inside Ω and satisfies the inhomogeneous boundary conditions from above. It is not hard to see that such a u_D indeed exists. For example, one can check that the following function meets these requirements

$$u_D(x, y) := (1 - x) \cdot y(1 - y) \cdot (1, 0)^T.$$

Using this, we set

$$u := \tilde{u} + u_D,$$

where (\tilde{u}, p) is the solution to the standard Stokes problem with homogeneous boundary conditions. Plugging this in to the already known formulation from (10) and using the bilinearity of a , we get

$$\begin{aligned} a((\tilde{u} + u_D, p), (v, q)) &= L(v) \iff a((\tilde{u}, p) + (u_D, 0), (v, q)) = L(v) \\ &\iff a((\tilde{u}, p), (v, q)) + a((u_D, 0), (v, q)) = L(v) \end{aligned}$$

Therefore, we get the following modified variational formulation: Find $(\tilde{u}, p) \in V \times Q$ satisfying

$$a((\tilde{u}, p), (v, q)) = \underbrace{L(v) - a((u_D, 0), (v, q))}_{=: \tilde{L}(v, q)}, \quad \forall (v, q) \in V \times Q, \quad (15)$$

where $u_D \in H^1(\Omega)^2$ is fixed satisfying both smoothness inside Ω as well as the boundary conditions (13) and (14). Note that, by construction, our right-hand side \tilde{L} now takes an additional argument compared the initial Stokes problem. With this, we are now at a point where we can formally state and prove our desired existence theorem.

Theorem 2.12 Let $V := \{v \in H^1(\Omega)^2 \mid v|_{\Gamma_L} = (1, 0)^T \text{ and } v|_{\Gamma_W} = (0, 0)^T\}$ and $Q := L^2(\Omega)$. Let $u_D \in H^1(\Omega)^2$ be fixed such that it is smooth inside Ω and satisfies the boundary conditions (13) and (14). Then, the stabilized variational formulation (10) of the Stokes problem admits a unique solution for every $\epsilon > 2C^2/\mu$.

Proof. We follow a similar line of proof as for Theorem 2.8, i.e., we want to apply Theorem 2.7 in order to prove the existence of (\tilde{u}, p) solving (15). With that, we then have that the composite term $u = \tilde{u} + u_D$, where $u_D \in H^1(\Omega)^2$ is smooth inside Ω and satisfies the boundary conditions (13) and (14) is indeed a solution of the usual variational formulation with inhomogeneous boundary conditions (by construction).

By the proof of Theorem 2.8, we already know that a is a continuous and coercive bilinear form. Hence, the only thing left to show is the continuity of the modified right-hand side \tilde{L} . Since it is constructed as the sum of the two continuous forms a and L , we may directly conclude that the same applies to \tilde{L} itself. Therefore, using Lax-Milgram, we get that there exists a unique pair $(\tilde{u}, p) \in H_0^1(\Omega)^2 \times Q$ solving (15). Hence, $(u, p) \in V \times Q$ is the unique solution to (10) for V and Q as stated in the assumptions. \square

2.4 Stokes Flow with Elliptical Obstacle

The second variation of the Stokes problem we want to consider is the *Stokes Flow with an elliptical obstacle*. The formal setting does not change much compared to the one considered in the section before. However, for the sake of completeness, we will state it here. Again, let $\Omega := (0, 1)^2 \subset \mathbb{R}^2$, $\mu := 1$ and consider

$$\begin{aligned} -\mu \Delta u + \nabla p &= f && \text{in } \Omega, \\ \operatorname{div}(u) &= 0 && \text{in } \Omega, \\ u &= (1, 0)^T && \text{on } \Gamma_L, \end{aligned} \quad (16)$$

$$u = (0, 0)^T \quad \text{on } \Gamma_W \cup \Gamma_E, \quad (17)$$

with $\Gamma_L := \{0\} \times (0, 1) \subset \partial\Omega$ and $\Gamma_W := (0, 1) \times \{0, 1\} \subset \partial\Omega$ denoting the left, top and bottom parts of the boundary $\partial\Omega$, respectively. The only change we introduce is an expansion of the zero boundary condition. From now on, we do not only want to avoid any velocity at the top and bottom of our domain but also on an elliptical obstacle located inside of the domain. For a general proof of existence of a solution to the weak formulation, the exact definition of said obstacle is negligible. Hence, we will denote it by $\Gamma_E \subset \subset \Omega$ without an explicit definition.

For this problem, we get the same variational formulation as before but again with a slightly altered velocity function space $V := \{v \in H^1(\Omega)^2 \mid v|_{\Gamma_L} = (1, 0)^T \text{ and } v|_{\Gamma_W \cup \Gamma_E} = (0, 0)^T\}$ together with an exemplary boundary function

$$u_D(x, y) := (1 - x) \cdot y(1 - y) \cdot \|(x, y) - P_{\Gamma_E}(x, y)\|_2^2 \cdot (1, 0)^T,$$

where P_{Γ_E} denotes the usual projection of a given pint (x, y) onto Γ_E . The proof of existence then works analogously to the one we discussed in [Theorem 2.12](#).

2.5 Lid-Driven Cavity

The third and last variation of the Stokes problem we elaborate on is the so-called *Lid-Driven Cavity*. Again the changes compared to the standard stokes flow are minor and only lay in the specification of different boundary conditions. The problem reads as follows: Let $\Omega := (0, 1)^2 \subset \mathbb{R}^2$, $\mu := 1$ and consider

$$\begin{aligned} -\mu \Delta u + \nabla p &= f && \text{in } \Omega, \\ \operatorname{div}(u) &= 0 && \text{in } \Omega, \\ u &= (0, 1)^T && \text{on } \Gamma_T, \end{aligned} \tag{18}$$

$$u = (0, 0)^T \quad \text{on } \partial\Omega \setminus \Gamma_T, \tag{19}$$

with $\Gamma_T := (0, 1) \times \{1\} \subset \partial\Omega$ denoting the top part of the boundary $\partial\Omega$, respectively. Analogous to before, this different Dirichlet boundary conditions do not affect the corresponding variational formulation directly but only the velocity space $V := \{v \in H^1(\Omega)^2 \mid v|_{\Gamma_T} = (0, 1)^T \text{ and } v|_{\partial\Omega \setminus \Gamma_T} = (0, 0)^T\}$ on which we want to solve said problem. A smooth boundary function which meets these restrictions is, for example,

$$u_D(x, y) := x(1 - x) \cdot y^2 \cdot (1, 0)^T.$$

Hence, one may again use a modified version of [Theorem 2.12](#) in order to prove the existence and uniqueness of a solution to said problem.

3 Finite Element Method

In the [Introduction](#), we already mentioned that the finite element method is a well established method for finding the solution of a given partial differential equation. Hence, in the following, we can build on this broad research and provide the reader with a short overview on the basics behind the implementation of this method using the Python package FEniCS.

In order to implement FEM for a given PDE, we start by computing its variational form (cf. (8) and (9)). The domain Ω from the initial PDE is discretized using a square or triangular mesh for a given fixed step size h . Over this mesh, we construct finite-dimensional subspaces $V_h \subset V$ (velocity space) and $Q_h \subset Q$ (pressure space) as well as a mixed space $W_h = V_h \times Q_h$. The latter concept is helpful for the computation of the solution of the given weak formulation using this package but does not impose any restrictions. For the sake of stability and accuracy, we choose the well-known Taylor-Hood

elements for the construction of these spaces (see [3, Chapter 3.4.3] for more information).

Taylor-Hood elements are crucial for the stability and convergence of mixed finite element methods for saddle-point problems like Stokes in practice. In the two-dimensional case, this means using piecewise quadratic (P2) basis functions for the velocity and piecewise linear (P1) functions for the pressure. The higher order velocity space allows for a finer approximation, which in turn stabilizes the dependence with the pressure field. In practice, from the mixed function space W , we consider test functions u_h and p_h together with trial functions v_h and q_h over the function spaces V_h and Q_h .

We then formulate the discrete problem: Find $(u_h, p_h) \in V_h \times Q_h$ such that for all $(v_h, q_h) \in V_h \times Q_h$, the variational equations hold, that is

$$\begin{aligned}\tilde{a}(u_h, v_h) + b(v_h, p_h) &= F(v_h), \quad \forall v_h \in V_h, \\ b(u_h, q_h) &= G(q_h), \quad \forall q_h \in Q_h,\end{aligned}$$

In order to use the solver included in the Python package FEniCS for this weak problem, we combine both equations into one coherent expression by adding together each respective side. In other words, we sum up all present bilinear forms on the left-hand side to obtain one single bilinear form and do the same for the linear forms on the right-hand side. This results in

$$\underbrace{\tilde{a}(u_h, v_h) + b(v_h, p_h) + b(u_h, q_h)}_{=:a((u_h, p_h), (v_h, q_h))} = \underbrace{F(v_h) + G(q_h)}_{=:L(v_h, q_h)}, \quad \forall (v_h, q_h) \in V_h \times Q_h$$

Analogously to [Section 2.2](#), we also equip a with a stabilization term for the pressure p . This is not only useful when it comes to proving the existence and uniqueness of a solution but also without it, p is (usually) only fixed up to a constant which makes a rigorous comparison of the different methods impossible. We will go into detail about this, when we consider the comparison for the different problems.

The associated boundary conditions of the problem are formalized using discrete functions for each side of the mesh. For our implementation, we avoided hard-coded boundary conditions and instead followed the idea behind the smooth boundary function $u_D \in H^1(\Omega)^2$ introduced in the sections before. Such a smooth approximation of the boundary not only prevents contradicting boundary conditions on the edges of the domain but also ensures a more realistic behaviour of the flow as well as the associated pressure. Using an internal function from FEniCS, those (smooth) boundary conditions are applied to the respective function spaces V_h and Q_h interpreted as subspaces of the mixed space W_h . Lastly, all of those separate boundary conditions are collected in a combined list which is then used as a separate argument when calling the solver of the weak formulation.

Said solver returns a combined solution $w_h = (u_h, p_h)$ inheriting both the velocity and the pressure. The separate components can then be extracted using a FEniCS function that splits w_h .

4 Physics-Informed Neural Networks

Compared to FEM, Physics-Informed Neural Networks (PINNs) are based on a fundamentally different idea for solving PDEs. Unlike FEM, they follow a mesh-free, data-driven approach. In other words, PINNs do not require meshing of the given domain into elements or defining basis functions with local support. Instead, the main idea is to represent the solution of a given problem as a neural network and to train it such that the governing equations and boundary conditions are satisfied.

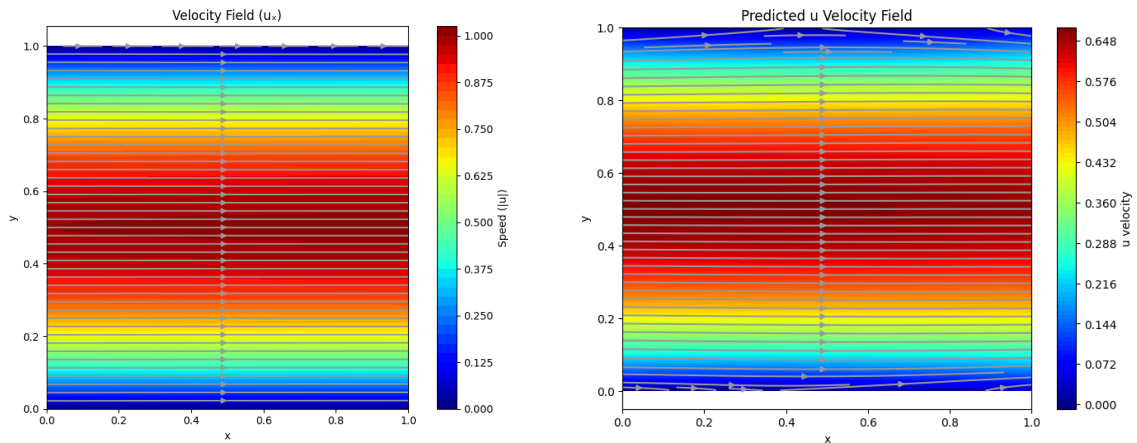
In our implementation for a given PDE, we start by defining sample points on our domain using a structured grid and converting it to a tensor, that is a generalized n -dimensional array. Note that one may also choose the points randomly, i.e., the points considered do not have to be equidistant. In this context, the use of a tensor enables conveniences such as automatic differentiation and GPU acceleration capabilities. Although the use of a grid might resemble meshing, the difference lies in the absence of any topological structure. That is, no connectivity and no basis functions are associated with these points. They merely serve as locations where the residuals of the PDE and the boundary conditions are evaluated. Coming back to our implementation, we split these points into two sets, one containing all interior points (where the PDE is enforced) and one consisting of the points that are located on the boundary of the domain (where the corresponding boundary conditions are imposed).

We then go over to defining the PINN model itself. In our case, we use a fully connected feedforward neural network that outputs the pressure and both of the velocity components separately. This facilitates further processing. Derivatives are computed using PyTorch's included automatic differentiation tool, allowing us to express the PDE equations directly as residuals involving gradients and Laplacians of the network output. We then use this to construct the loss function. Since the problems we consider are all variants of the Stokes problem, said loss function consists of the momentum equation residuals and the divergence (incompressibility) residuals (both at interior points) and the residual resulting from the boundary conditions. Analogously to our implementation of FEM, we consider a stabilization term for the pressure p . Further, we also implement our boundary conditions using the same smooth boundary function $u_D \in H^1(\Omega)^2$. This comes with the same advantages as for FEM and additionally ensures comparability of the results from both methods in the sections to follow.

The network is trained using stochastic optimization, that is, the so-called *Adam* solver. By construction of our loss functional, all boundary constraints are enforced through their associated residuals. With this, the PINN approximates the solution by repeatedly and further minimizing said function. In practice, a fixed number of iterations is defined (epochs). After the last run, one gets the final approximation of the solution through the current value of the respective components. Note that when it comes to comparing the result with the one produced by other methods like FEM, the velocity u is only available as separate components and one may need to reassemble it accordingly, depending on the desired comparison.

5 Comparison

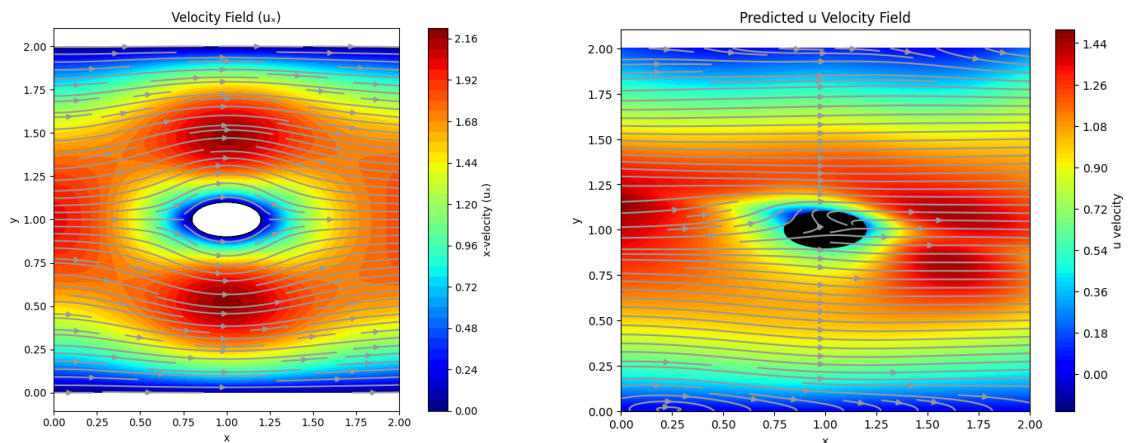
We now shift our attention on the practical comparison of both FEM and PINNs using the PDEs introduced in the sections before. As we have already proven the existence and uniqueness of solutions for each respective weak formulation, we can rely on that and only focus on the quality of the solutions produced by both solution methods. First, we take a look at the streamline diagrams of the velocity as well as the diagrams of the corresponding pressure produced by both methods for each problem side by side. We do this in order to get an initial sense of the general accuracy of the computations.



(a) Streamline diagram produced by FEM

(b) Streamline diagram produced by PINN

Figure 5.1: Velocity of the Stokes problem with inhomogeneous boundary conditions

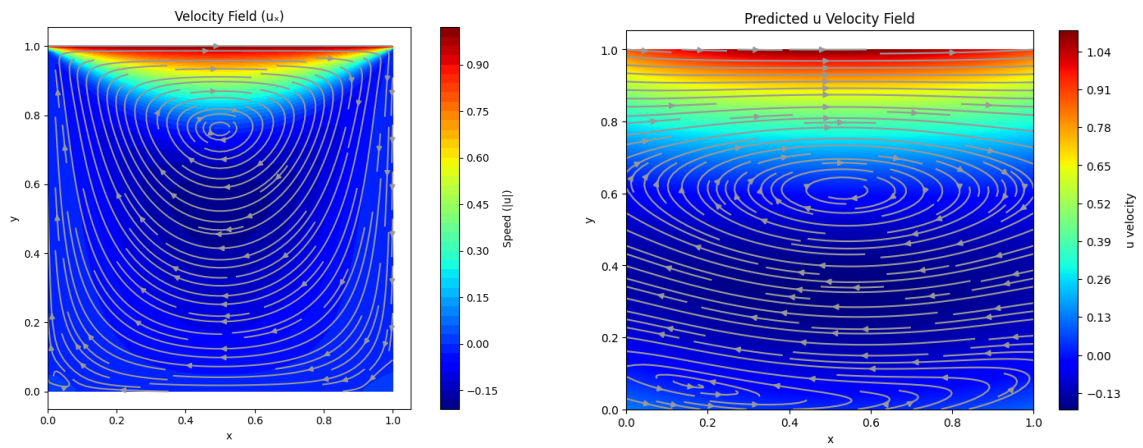


(a) Streamline diagram produced by FEM

(b) Streamline diagram produced by PINN

Figure 5.2: Velocity of the Stokes problem with elliptical obstacle

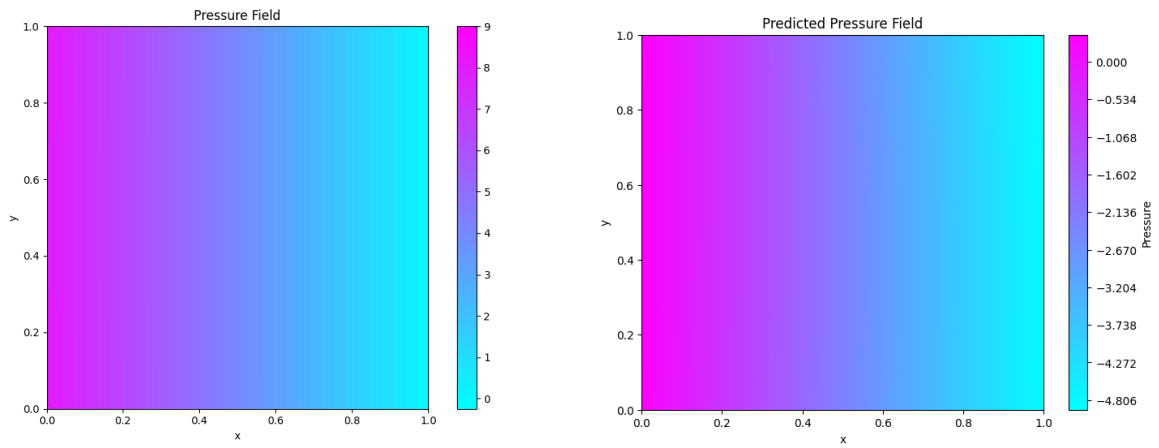
In the following, we compare both methods from a numerical point of view. That is, we take the error between the methods as well as the convergence behaviour into consideration. Since we do not have analytical solutions for any of the given problems, we take the estimations produced by the Finite Element Method as the desired state of each respective problem. In other words, we take a look at the solution of the Physics-Informed



(a) Streamline diagram produced by FEM

(b) Streamline diagram produced by PINN

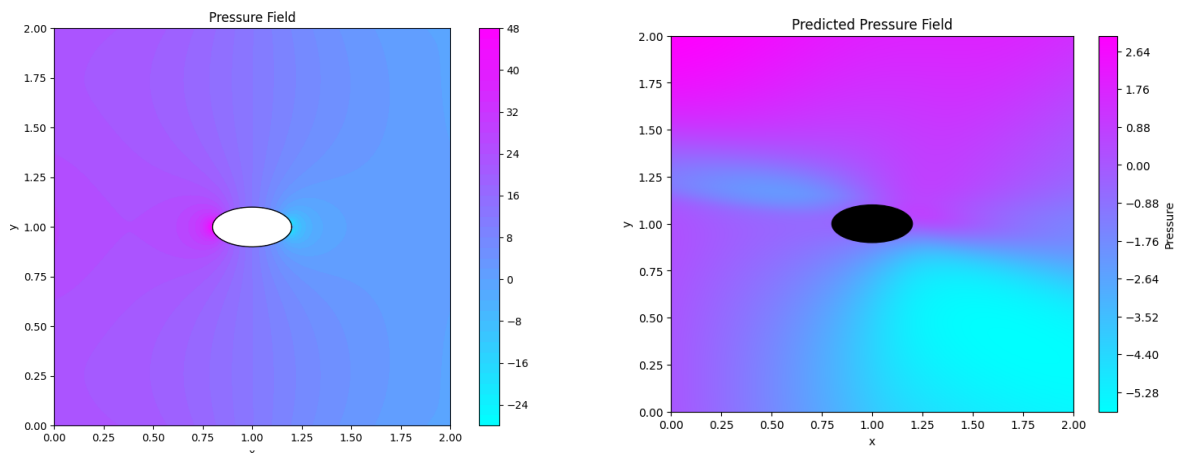
Figure 5.3: Velocity of the Lid-Driven Cavity



(a) Pressure diagram produced by FEM

(b) Pressure diagram produced by PINN

Figure 5.4: Pressure of the Stokes problem with inhomogeneous boundary conditions



(a) Pressure diagram produced by FEM

(b) Pressure diagram produced by PINN

Figure 5.5: Pressure of the Stokes problem with elliptical obstacle

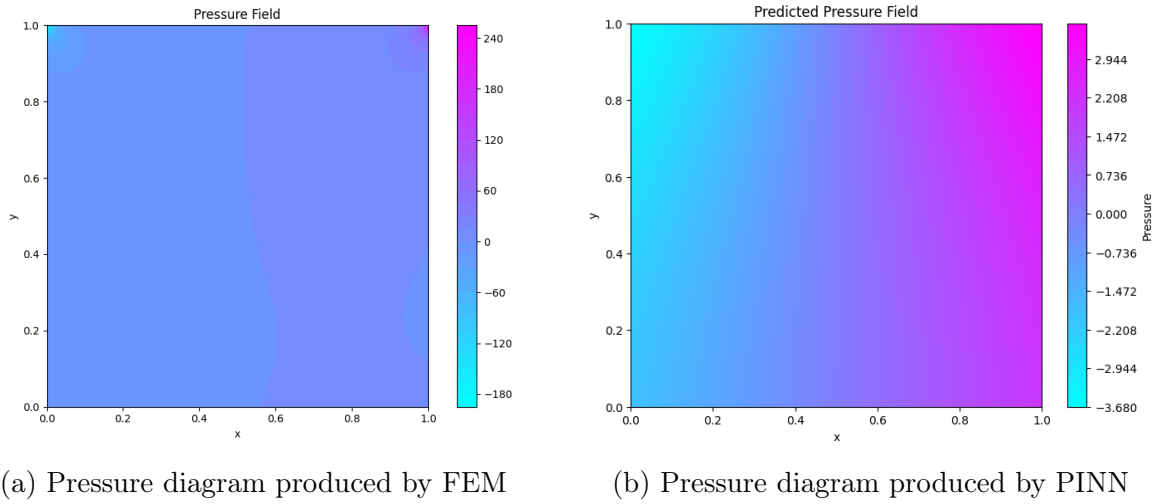


Figure 5.6: Pressure of the Lid-Driven Cavity

Neural Network and compute the L^2 -error with regard to the solution provided by FEM. We do this for different sizes of the mesh and collect the results in [Table 1](#) and [Table 2](#) for the velocity and the pressure part, respectively.

N	L^2 -norm for problem 1	L^2 -norm for problem 2	L^2 -norm for problem 3
8	3.973	6.786	4.478
16	4.004	4.279	4.417
32	3.891	4.730	4.503
64	3.996	5.011	4.425
128	3.979	4.989	4.479

Table 1: Comparison of the L^2 -error $\|u_{FEM} - u_{PINN}\|_2$ of the velocity u of both methods for different mesh sizes.

N	L^2 -norm for problem 1	L^2 -norm for problem 2	L^2 -norm for problem 3
8	28.633	36.754	15.737
16	26.735	30.949	17.482
32	28.850	34.895	16.860
64	28.276	36.193	17.003
128	28.480	36.896	17.290

Table 2: Comparison of the L^2 -error $\|p_{FEM} - p_{PINN}\|_2$ of the pressure p of both methods for different mesh sizes.

At first glance, both methods seem to produce somewhat similar results. However, when it comes to the critical parts of the mesh (e.g., the top and bottom boundary of [Figure 5.1](#) or [Figure 5.2](#) or the center of [Figure 5.3](#)) the solutions resulting from PINN show to be significantly worse than the ones from FEM. Especially at the boundaries of the mesh or an obstacle in the middle (cf. [Figure 5.2](#)), PINNs seem to difficulties meeting said conditions. The result mostly blurs over the obstacle which also translates over into the

differences with regard to pressure diagrams (cf. [Figure 5.4](#), [Figure 5.5](#) and [Figure 5.6](#)). Additionally, those differences become even more apparent from the numerical standpoint. While the L^2 -error between the respective velocity is already quite large, said difference only increases with regard to the error of the pressure functions. Again, this can be traced back to the difficulties of PINNs for the given boundary conditions.

In general, for the Finite Element Method, both velocity and pressure fields are computed within rigorously defined function spaces, ensuring that the numerical solutions strictly satisfy the incompressibility constraint and boundary conditions. This leads to stable, well-behaved solutions where the pressure is determined up to a constant (or fixed by a normalization condition), and velocity satisfies physical constraints such as no-slip or inflow/outflow profiles exactly. In contrast, PINNs approximate both velocity and pressure with neural networks, where the governing equations and boundary conditions are enforced weakly through the loss function. Boundary conditions are not imposed exactly but rather penalized during training, which can lead to smoother velocity fields near boundaries but may also cause deviations from physical constraints. Similarly, the pressure field in PINNs is learned indirectly and often lacks the physical boundedness and normalization typically ensured in FEM. This can result in drift or artificial pressure gradients, especially near obstacles or sharp features in the domain.

6 Conclusion

As we have seen throughout this paper, especially in [Section 5](#), there is a justified reason to doubt the consideration of PINNs as a serious alternative to FEM when it comes to solving PDEs. Even for rather simple problems as we have elaborated on in [Section 2](#), the solution computed by PINNs remains significantly worse compared to the one resulting from FEM. This not only becomes apparent when looking at the respective graphs for each of the given problems, but even more so when comparing the exact numerical difference of the solutions provided by both methods. Regardless of the used mesh size, PINNs generally deviate considerably from FEM. Especially at those boundaries where certain conditions must be enforced, PINN reaches its limit and the computed solution often hardly ever meets said conditions.

Even if it was the case that PINNs return similar solutions to the ones provided by FEM, favouring the first method still remains questionable: when it comes to computational performance, the comparison of these methods becomes rather difficult and less meaningful. While FEM tends to use much more RAM, PINNs take way longer to train and compute a solution. The latter is explained by the fact that PINNs do not solve the problem directly but rely on the training of a model to do so which consequently takes longer than solving it once. All in all, if one is in the position to already have a well trained PINN at hand, this solution method may indeed be preferred over FEM. However, since training such a model requires careful tuning in order to be well posed, the challenge lies in obtaining such a well trained model in the first place.

References

- [1] Daniele Boffi, Franco Brezzi, and Michel Fortin. *Mixed Finite Element Methods and Applications*. 1. Springer Berlin, Heidelberg, 2013. ISBN: 978-3-642-36518-8. DOI: <https://doi.org/10.1007/978-3-642-36519-5>.
- [2] Jean-Michel Bony. *Cours d'analyse: théorie des distributions et analyse de Fourier*. Editions Ecole Polytechnique, 2001. ISBN: 2730207759, 9782730207751.
- [3] Hans Petter Langtangen and Anders Logg. *Solving PDEs in Python*. 1. Springer Cham, 2017. ISBN: 978-3-319-52462-7. DOI: <https://doi.org/10.1007/978-3-319-52462-7>.
- [4] Anders Logg, Kent-Andre Mardal, and Garth Wells. *Automated Solution of Differential Equations by the Finite Element Method*. 1. Springer Berlin, Heidelberg, 2012. DOI: [10.1007/978-3-642-23099-8](https://doi.org/10.1007/978-3-642-23099-8).
- [5] Alberto Valli. *Weak Derivatives and Sobolev Spaces*. 154. Springer, Cham, 2023. ISBN: 978-3-031-35976-7. DOI: https://doi.org/10.1007/978-3-031-35976-7_4.